

IDENTIFICATION OF HEAT AND VAPOR TRANSFER COEFFICIENTS, EQUIVALENT AIR TEMPERATURES, AND VAPOR PRESSURES FOR LOCAL BODY SEGMENTS IN NONUNIFORM THERMAL ENVIRONMENTS

*Tomonori SAKOI¹, Shinsuke KATO², Ryozo OOKA²,
Hideaki NAGANO², Shengwei ZHU³, and Toshiaki OMORI⁴*

¹*Shinshu University, Ueda, JAPAN,* ²*Tokyo University, Tokyo, JAPAN,*
³*Harvard University, Boston, USA,* ⁴*Tokyo Gas Co., Ltd., Tokyo, JAPAN*

Contact person: *Tomonori SAKOI* (t-sakoi@shinshu-u.ac.jp)

INTRODUCTION

Heating and refrigerating systems are designed to achieve an appropriate thermal physiological state of the human body. In order to predict the thermal physiological state of the human body in an evaluated environment, Zhu et al. 2008 developed a method of coupled analysis of computational fluid dynamics (CFD), human thermal model (Sakoi et al. 2006), and radiation such as that measured using the Monte Carlo method (Omori et al. 2004). In addition to Sakoi et al.'s human thermal model, there exist many human thermal models (e.g., Stolwijk 1971) that can be used in similar coupled analyses. Despite the similar models used in the CFD and radiation analysis, the predicted thermal physiological state differs with the human thermal model used in the coupled analysis. Moreover, due to the influence of heat transfer among the body parts by blood flow, the difference among the multi-segmental human thermal models becomes clear.

The local thermal physiological state is an important factor for thermal comfort in a nonuniform thermal environment (e.g., Zhang et al. 2004). Despite the differences in the predicted results of the local thermal physiological state among models, all human thermal models determine the local thermal physiological state by a common mechanism, i.e., heat balances in the body tissues. In order to obtain effective results from the coupled analysis of CFD and radiation for all human thermal models, in this study, we propose a rational method to define the following in a nonuniform thermal environment: (a) equivalent local air temperatures ($T_{a,i}$), (b) equivalent local vapor pressures ($P_{a,i}$), (c) local convective heat transfer coefficients ($h_{c,i}$), and (d) local latent heat transfer coefficient ($h_{e,i}$). These parameters can be commonly used as inputs for all human thermal models. However, since environmental nonuniformity makes it difficult to determine $T_{a,i}$ and $P_{a,i}$, thus far, it has been difficult to define reasonable values of $T_{a,i}$, $P_{a,i}$, $h_{c,i}$, and $h_{e,i}$. This is a novel study to identify the abovementioned parameters in a nonuniform thermal environment by CFD; however, it was difficult to determine the values of $T_{a,i}$ and $P_{a,i}$ among these.

METHODS

It is possible to obtain local convective and latent heat fluxes by means of CFD when the local outer surface temperatures ($T_{s,i}$) and vapor pressures ($P_{s,i}$) are specified for a local part i in an

environment. In order to define $T_{a,i}$, $P_{a,i}$, $h_{c,i}$, and $h_{e,i}$ of the environment, we carry out various analyses of the environment using a few combinations of $T_{s,i}$ and $P_{s,i}$. We obtain the local convective heat flux ($Q_{c,i1}$) and local evaporative (latent) heat flux ($Q_{e,i1}$) in one CFD analysis by using $T_{s,i1}$ and $P_{s,i1}$ as the boundary conditions of the human body surface. Similarly, we obtain the values of $Q_{c,i2}$ and $Q_{e,i2}$ for $T_{s,i2}$ and $P_{s,i2}$ in other analyses. The difference between the values of $T_{s,i1}$ and $T_{s,i2}$ and those of $Q_{c,i1}$ and $Q_{c,i2}$ can be substituted in Eq. (1) to determine the local convective heat transfer coefficient ($h_{c,i}$). Here, $h_{c,i}$ is the difference in the convective heat transfer rate caused by a 1°C variation in $T_{s,i}$ in the environment.

$$h_{c,i} = \frac{Q_{c,i1} - Q_{c,i2}}{T_{sk,i1} - T_{sk,i2}} \quad (1)$$

The equivalent local air temperature ($T_{a,i}$) can be determined from the obtained values of $h_{c,i}$, $Q_{c,i1}$, $Q_{c,i2}$, $T_{s,i1}$, and $T_{s,i2}$ as shown in Eq. (2). For a fixed value for $h_{c,i}$ that can be determined for the environment, $T_{a,i}$ is the local air temperature that results in $Q_{c,i1}$ and $Q_{c,i2}$ for $T_{s,i1}$ and $T_{s,i2}$, respectively.

$$T_{a,i} = \frac{T_{sk,i1} \cdot Q_{c,i2} - T_{sk,i2} \cdot Q_{c,i1}}{Q_{c,i2} - Q_{c,i1}} \left(= T_{sk,i1} - \frac{Q_{c,i1}}{h_{c,i}} = T_{sk,i2} - \frac{Q_{c,i2}}{h_{c,i}} \right) \quad (2)$$

Similarly, $h_{e,i}$ and $P_{a,i}$ are defined by Eqs. (3) and (4), respectively. Here, $h_{e,i}$ is the difference in the latent heat transfer rate caused by a difference of 1 kPa in $P_{s,i}$ in the environment, and $P_{a,i}$ is the local vapor pressure that results in $Q_{e,i1}$ and $Q_{e,i2}$ for $P_{s,i1}$ and $P_{s,i2}$, respectively, when the fixed $h_{e,i}$ can be determined for the environment.

$$h_{e,i} = \frac{Q_{e,i1} - Q_{e,i2}}{P_{sk,i1} - P_{sk,i2}} \quad (3)$$

$$P_{a,i} = \frac{P_{s,i1} \cdot Q_{e,i2} - P_{s,i2} \cdot Q_{e,i1}}{Q_{e,i2} - Q_{e,i1}} \left(= P_{s,i1} - \frac{Q_{e,i1}}{h_{e,i}} = P_{s,i2} - \frac{Q_{e,i2}}{h_{e,i}} \right) \quad (4)$$

Our concept for calculating $T_{a,i}$, $P_{a,i}$, $h_{c,i}$, and $h_{e,i}$ is similar to that using an experimental thermal manikin (Kohri et al. 1995) for calculating the local combined heat transfer coefficients and local operative temperatures.

For the application of our concept, we estimated $T_{a,i}$, $P_{a,i}$, $h_{c,i}$, and $h_{e,i}$ in an asymmetric radiant field from the front and back (Zhu et al. 2008) of a human subject. Fig. 1 shows the field to be

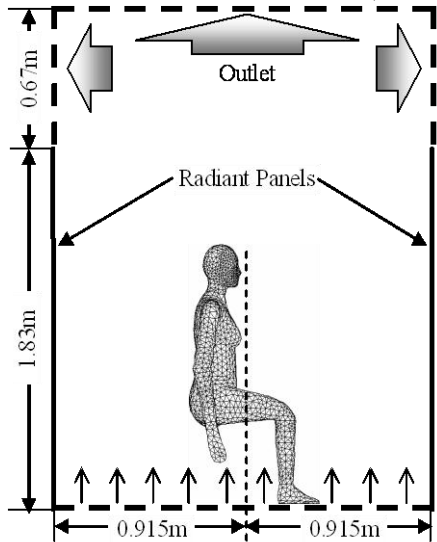


Fig.1 Field to be analyzed

Table 1 Boundary settings of human body surface

No.	1	2	3	4
$T_{sk,i}$ [°C]	33.3	33.3	33.8	33.8
$P_{sk,i}$ [kPa]	2.046 [†]	3.683	2.046	3.683 [†]

[†]2.046 kPa corresponds to 40% RH at 33.3 °C, and 3.683 kPa corresponds to 70% RH at 33.8 °C.

Table 2 Combinations of boundary conditions for human body for identifying $T_{a,i}$, $P_{a,i}$, $h_{c,i}$, and $h_{e,i}$

Descriptions in Figs. 4–6	Combinations of “No.” in Table 1	Variables to be identified
T_{sk} 33.3	Cases 1 and 2	$P_{a,i}$ and $h_{e,i}$
T_{sk} 33.8	Cases 3 and 4	$P_{a,i}$ and $h_{e,i}$
P_{sk} 40 RH	Cases 1 and 3	$T_{a,i}$ and $h_{c,i}$
P_{sk} 70 RH	Cases 2 and 4	$T_{a,i}$ and $h_{c,i}$

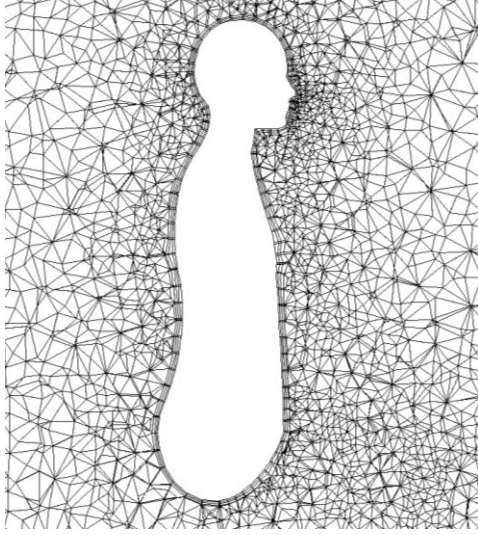


Fig. 2 Cells around human body model

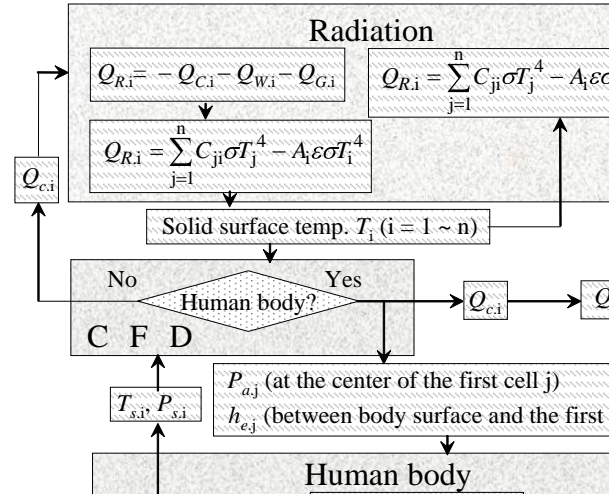


Fig. 3 Flowchart of coupled analysis

analyzed. We asked a human subject wearing only shorts to get into the sitting posture. Air at 28 °C and 40% RH flowed into the field from the floor at a uniform velocity of 0.05 m/s. The air outlet was provided on the upper part of the four walls and the ceiling. Except for the inlet (floor), outlet, and radiant panels, the environmental boundary was set to be adiabatic. The temperatures of the front and back radiant panels were set to 14 °C and 42 °C, respectively.

For the CFD analysis, we used commercial software (Star-CD) and estimated the heat and mass fluxes using a low-Re-number k- ϵ turbulence model (Lien et al. 1996) with the SIMPLE algorithm and the monotone advection and reconstruction scheme (MARS, a second-order scheme) (van Leer 1979) for convection terms. For the radiation analysis, we used the Monte Carlo method incorporating the symmetrization proposed by Omori et al. 2004. Table 1 shows the boundary conditions for a human body surface. We carried out four analyses corresponding to the boundary conditions listed in Table 1. In order to consider the effect of the shorts and the hair on the human body, we added local effective resistances with heat and vapour transfers on the head, waist, and thighs of the subject.

As shown in Fig. 2, the first three cell layers over the surface of the human body had prismatic-shaped fluid cells, while the rest of the flow field was filled with tetrahedral meshes. In the analyses, 14,632 triangular surface meshes and 285,199 spatial cells were used. Fig. 3 shows the flowchart of the coupled analysis. The CFD outputted the convective heat flux ($Q_{c,i}$) for each surface and the vapor pressure ($P_{a,j}$) at the center of the first cell and the latent heat transfer coefficients ($h_{e,j}$) between $P_{a,j}$ and the skin surface. The radiation analysis outputted solid surface temperatures of the surfaces (except for the human body) to the CFD. Despite our using the fixed $T_{sk,i}$ and $P_{sk,i}$ (listed in Table 1) in the current analysis, when $T_{sk,i}$, $P_{sk,i}$, and local latent heat flux ($E_{sk,i}$) were analyzed using a human thermal model (results of which are present in the section RESULTS), we input $Q_{c,i}$, $P_{a,j}$, and $h_{e,j}$ obtained from the CFD analysis and the radiative heat transfer rate ($Q_{R,i}$) obtained from the radiation analysis into the human thermal model. Thereon, $T_{sk,i}$ and $P_{sk,i}$, and $E_{sk,i}$, $T_{s,i}$, and $P_{s,i}$ were calculated using the human thermal model and transferred to the CFD. Through these analyses, we obtained steady $Q_{c,i}$ and $Q_{e,i}$. Table 2 lists combinations of $T_{sk,i}$ and $P_{sk,i}$ to identify the objective values ($T_{a,i}$, $P_{a,i}$, $h_{c,i}$, and $h_{e,i}$). In order to separate the influences of the sensible heat transfer and latent heat transfer, we identified $T_{a,i}$ and $h_{c,i}$ from the results obtained at the same $P_{sk,i}$. Further, we also identified $P_{a,i}$ and $h_{e,i}$ from the results obtained at the same $T_{sk,i}$.

RESULTS

Fig. 4 and Fig 5 show the identified $T_{a,i}$, $P_{a,i}$, $h_{c,i}$, and $h_{e,i}$. Both the combination of $P_{sk}40$ RH (listed in Table 2) and that of $P_{sk}70$ RH resulted in similar distributions in $T_{a,i}$, and $h_{c,i}$. Similarly, both the combination of $T_{sk}33.3$ and that of $T_{sk}33.8$ resulted in similar distributions in $P_{a,i}$, and $h_{e,i}$. Since there exists a similarity rule between convective heat transfer and latent heat transfer, $h_{c,i}$ and $h_{e,i}$ have similar distributions for the body parts. The distribution of $T_{a,i}$ was due to the environmental nonuniformity. $T_{a,i}$ on the front side of the legs and forearms tended to be lower than that on the back side. Fig. 6 shows a comparison of the distribution of $T_{sk,i}$ obtained from the coupled analysis of CFD radiation analyses and our human thermal model (Sakoi et al. 2006) with that obtained from the same human thermal model and the identified $T_{a,i}$, $P_{a,i}$, $h_{c,i}$, $h_{e,i}$, local radiative heat transfer coefficients, and local mean radiant temperatures that were determined in the same manner. Since similar distributions were obtained, we concluded that sufficient accuracy was achieved for the predicted local physiological states obtained from the identified $T_{a,i}$, $P_{a,i}$, $h_{c,i}$, $h_{e,i}$, and a human thermal model as compared to those calculated by the coupled analysis of CFD and radiation analyses and the same human thermal model.

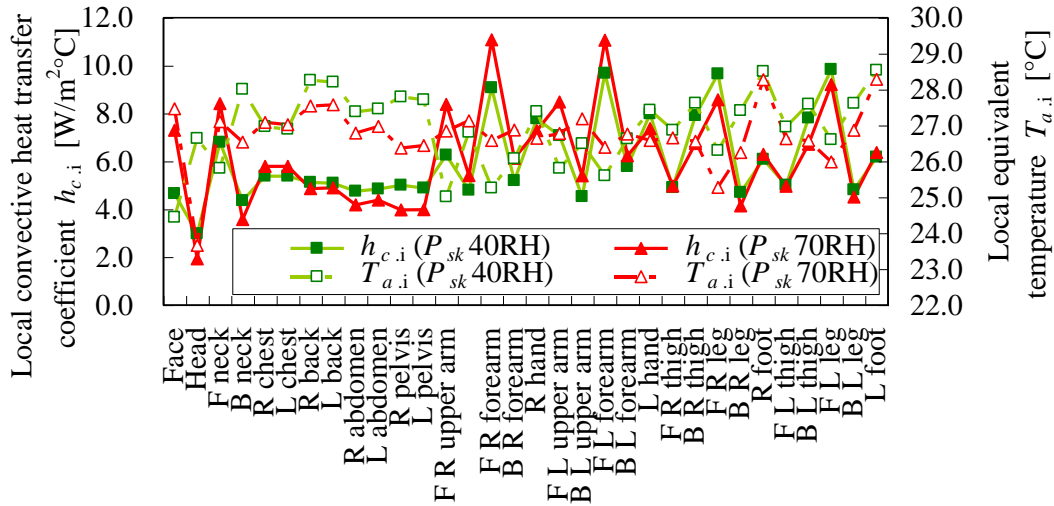


Fig. 4 Identified $T_{a,i}$ and $h_{c,i}$

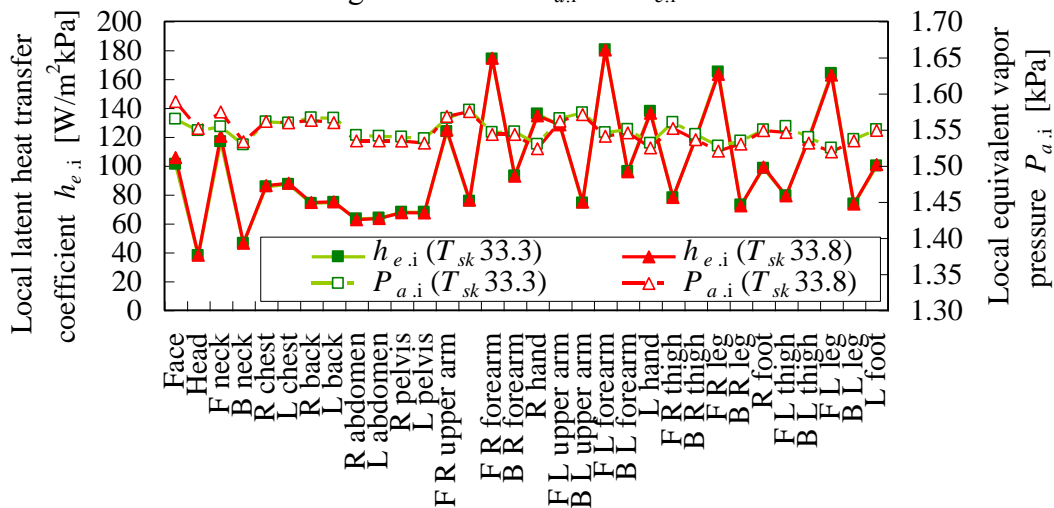


Fig. 5 Identified $P_{a,i}$ and $h_{e,i}$

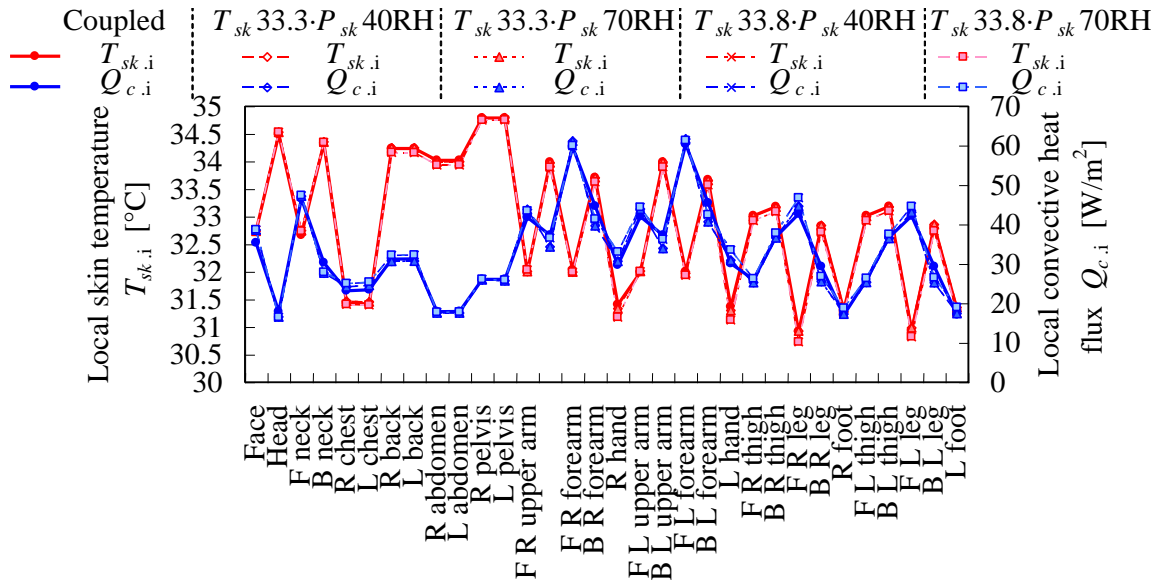


Fig. 6 Comparison of $T_{sk,i}$ and $C_{c,i}$ between coupled analysis and analysis using $T_{a,i}$, $P_{a,i}$, $h_{c,i}$, $h_{e,i}$

CONCLUSIONS

In this study, we proposed a method to define local equivalent air temperature ($T_{a,i}$), local equivalent vapor pressure ($P_{a,i}$), local convective heat transfer coefficient ($h_{c,i}$), and local vapor transfer coefficient ($h_{e,i}$) by numerical simulation. Our method can be used to rationally determine these parameters even in a nonuniform thermal environment. Since the obtained parameters can be used as inputs to many human thermal models, our method has the advantage that it can analyze the distribution of thermal physiological states of different human thermal models from limited results of coupled CFD and radiation analyses.

ACKNOWLEDGMENTS

This study was partially supported by a Grant-in-Aid for Scientific Research from the Ministry of Education, Culture, Sports, Science and Technology (MEXT), Japan (No.20360259)

REFERENCES

- Kohri I, T Kataoka, Y Fusada 1995. Evaluation method of thermal comfort in a vehicle by SET* using thermal manikin and theoretical thermoregulation model in man. IMechE Paper C496/022
- Lien FS, WL Chen, MA Leschziner 1996. Low-Reynolds-number eddy-viscosity modelling based on non-linear stress-strain/vorticity relations. Proceedings of 3rd Symposium on Engineering Turbulence Modelling and Measurement, pp.1–10
- Omori T, JH Yang, S Kato, S Murakami 2004. Coupled simulation of convection and radiation on thermal environment around an accurately shaped human body. Proceedings of the 9th International Conference on Air Distribution in Rooms
- Sakoi T, K Tsuzuki, S Kato, R Ooka, D Song, SW Zhu 2006. A three-dimensional human thermal model for non-uniform thermal environment. The 6th International Thermal Manikin and Modeling Meeting, pp.77–88
- Stolwijk JAJ 1971. A mathematical model of physiological temperature regulation in man. NASA Contractor Report 1855
- van Leer 1979. Toward the ultimate conservation difference scheme II: Monotonicity and conservation combined in a second order scheme. Journal of Computational Physics, Vol. 32, pp.101–136
- Zhang H, C Huizenga, E Arens, D Wang 2004. Thermal sensation and comfort in transient non-uniform thermal environments, European Journal of Applied Physiology Vol. 92, pp.728–733
- Zhu SW, S Kato, R Ooka, T Sakoi, K Tsuzuki 2008. Development of a computational thermal manikin applicable in a non-uniform thermal environment - Part 2: Coupled simulation using Sakoi's human thermal physiological Model, ASHRAE HVAC & R Research Vol.14 (4), pp.545–564